T lymphocytes and fractalkine contribute to myocardial ischemia/reperfusion injury in patients

Stephen E. Boag,[1] Rajiv Das,[2] Evgeniya V. Shmeleva,[1] Alan Bagnall,[2,3] Mohaned Egred,[2,3] Nicholas Howard,[4] Karim Bennaceur,[1] Azfar Zaman,[2,3] Bernard Keavney,[1,5] and Ioakim Spyridopoulos[1,2]

[1]Institute of Genetic Medicine, Newcastle University, Newcastle upon Tyne, United Kingdom. [2]Department of Cardiology, Freeman Hospital, Newcastle upon Tyne, United Kingdom. [3]Institute of Cellular Medicine, Newcastle University, Newcastle upon Tyne, United Kingdom. [4]University of Sunderland, Sunderland, United Kingdom. [5]Institute of Cardiovascular Sciences, The University of Manchester, Manchester, United Kingdom.

BACKGROUND. Lymphocytes contribute to ischemia/reperfusion (I/R) injury in several organ systems, but their relevance in ST elevation myocardial infarction (STEMI) is unknown. Our goal was to characterize lymphocyte dynamics in individuals after primary percutaneous coronary intervention (PPCI), assess the prognostic relevance of these cells, and explore mechanisms of lymphocyte-associated injury.

METHODS. Lymphocyte counts were retrospectively analyzed in 1,377 STEMI patients, and the prognostic relevance of post-PPCI lymphopenia was assessed by Cox proportional hazards regression. Blood from 59 prospectively recruited STEMI patients undergoing PPCI was sampled, and leukocyte subpopulations were quantified. Microvascular obstruction (MVO), a component of I/R injury, was assessed using MRI.

RESULTS. In the retrospective cohort, lymphopenia was associated with a lower rate of survival at 3 years (82.8% vs. 96.3%, lowest vs. highest tertile; hazard ratio 2.42). In the prospective cohort, lymphocyte counts fell 90 minutes after reperfusion, primarily due to loss of T cells. $CD8^+$ T cells decreased more than $CD4^+$ T cells, and effector subsets exhibited the largest decline. The early decrease in effector T cell levels was greater in individuals that developed substantial MVO. The drop in T cell subsets correlated with expression of the fractalkine receptor CX3CR1 ($r^2 = 0.99$, $P = 0.006$). Serum fractalkine concentration peaked at 90 minutes after reperfusion, coinciding with the T cell count nadir.

CONCLUSIONS. Lymphopenia following PPCI is associated with poor prognosis. Our data suggest that fractalkine contributes to lymphocyte shifts, which may influence development of MVO through the action of effector T cells.

TRIAL REGISTRATION. Not applicable.

FUNDING. British Heart Foundation (FS/12/31/29533) and National Institute of Health Research (NIHR) Newcastle Biomedical Research Centre.

Introduction

Primary percutaneous coronary intervention (PPCI) is now standard of care for the treatment of acute ST elevation myocardial infarction (STEMI). Although PPCI results in reduction in both mortality and morbidity compared with thrombolytic therapy, ischemia/reperfusion (I/R) injury remains an important complication, contributing up to 50% of final infarct size (1). I/R injury is a multifactorial process, to which metabolic factors (2), inflammation (3), and microvascular obstruction (MVO) (4) contribute. To date, no treatments targeting this process have shown conclusive benefit.

While the role of T lymphocytes (T cells) in I/R injury relating to other organ systems has been well studied (5), relatively little evidence exists concerning myocardial I/R injury. Two studies by Yang et al. have suggested a critical role for IFN-γ–producing $CD4^+$ T cells in a mouse model of myocardial I/R injury (6, 7). However, the significance of these cells in human patients undergoing PPCI for STEMI has yet to be studied.

While their specific contribution is not currently understood, indirect evidence points to a role for lymphocytes in myocardial infarction (MI) and I/R injury in humans. Several studies have identified poor prognostic significance of lymphopenia (8) or high neutrophil/lymphocyte ratio (9–13), although the type of infarct and treatment strategy have been variable. Furthermore, one study has identified a correlation between lymphopenia and MVO following PPCI (14). The goal of our study was to assess the prognostic impact of transient lymphopenia in a well-defined population undergoing PPCI for STEMI, clarify the subpopulations of cells involved, and investigate possible mechanisms.

Results

Lymphopenia after PPCI predicts long-term mortality. First, we wanted to determine whether lymphopenia predicted outcome in a well-defined population of STEMI patients undergoing PPCI. We retrospectively analyzed the lymphocyte counts of 1,377 consecu-

Conflict of interest: The authors have declared that no conflict of interest exists.
Submitted: November 17, 2014; **Accepted:** May 28, 2015.
Reference information: *J Clin Invest*. 2015;125(8):3063–3076. doi:10.1172/JCI80055.

Table 1. Baseline data for 1,377 patients included in retrospective analysis of mortality data

	Minimum lymphocyte tertile				
	Low (<1,300 cells/μl)	Middle (1,300–1,910 cells/μl)	High (>1,910/μl)	*n*	*P* value
Age (yr)	68.1 ± 13.5	62.1 ± 12.9	58.3 ± 11.7	1,377	<0.001
Male	327 (71.2)	329 (71.1)	336 (73.2)	1,377	0.785
BMI	26.6 ± 5.1	27.7 ± 5.2	28.3 ± 5.4	1,222	<0.001
Diabetes mellitus	51 (11.2)	42 (9.2)	51 (11.1)	1,375	0.526
Family history of CAD	168 (42.7)	183 (43.4)	202 (47.5)	1,240	0.32
Hypertension	206 (44.9)	184 (40.1)	163 (35.5)	1,377	0.015
Hypercholesterolemia	131 (28.5)	137 (29.8)	138 (30.1)	1,377	0.861
Current or ex-smoker	270 (63.5)	312 (70.7)	382 (86.0)	1,310	<0.001
Previous angina	114 (25.2)	79 (17.6)	95 (21.1)	1,352	0.019
Previous PCI	39 (8.5)	34 (7.4)	20 (4.4)	1,374	0.034
Previous MI	82 (18.4)	66 (14.8)	46 (10.1)	1,347	0.002
Previous CVA or TIA	34 (7.4)	17 (3.7)	16 (3.5)	1,377	0.008
PVD	15 (3.3)	18 (3.9)	13 (2.8)	1,377	0.653
Door to balloon time (min)	30.9 ± 18.5	29.3 ± 18.5	28.5 ± 17.5	1348	0.152
Total ischemic time (min)	276.4 ± 366.8	247.4 ± 238.2	283.6 ± 487.1	1329	0.320
Cardiogenic shock	22 (4.8)	8 (1.7)	10 (2.2)	1,367	0.012
Anterior MI	205 (44.9)	174 (38.3)	155 (33.9)	1,368	0.003
Multivessel PCI	65 (14.2)	41 (8.9)	40 (8.7)	1,377	0.01
TIMI 3 post-PCI	382 (89)	401 (93)	420 (95.2)	1,301	0.002
Hemoglobin (g/l)	135.8 ± 17.1	139.7 ± 16.8	143.0 ± 14.9	1374	<0.001
Serum cholesterol (mmol/l)	4.7 ± 1.3	5.1 ± 1.3	5.3 ± 1.3	1283	<0.001
Serum creatinine (μmol/l)	113.3 ± 69.0	98.8 ± 24.1	96.1 ± 22.2	1373	<0.001
Statin	399 (86.9)	416 (90.6)	423 (92.2)	1377	0.026
ACE inhibitor/ARB	374 (81.5)	407 (88.7)	410 (89.3)	1377	0.001
Beta-blocker	366 (79.7)	392 (85.4)	400 (87.1)	1377	0.006
Clopidogrel	404 (88.0)	420 (91.5)	428 (93.2)	1377	0.019
Aspirin	406 (88.5)	421 (91.7)	429 (93.5)	1377	0.025
Glycoprotein IIb/IIIa inhibitor	351 (76.8)	395 (86.6)	405 (88.4)	1371	<0.001

Continuous variables expressed as mean ± SD and compared using one-way ANOVA; categorical variables as *n* (%) and compared using χ^2 test. CAD, coronary artery disease; CVA, cerebrovascular accident; TIA, transient ischemic attack; PVD, peripheral vascular disease; ACE, angiotensin-converting enzyme; ARB, angiotensin II receptor blocker. "Diabetes mellitus" refers to types 1 and 2.

tive patients treated in a single tertiary center in the United Kingdom between April 2008 and February 2010 and discharged alive (see Table 1 for baseline characteristics). In particular, the minimum lymphocyte count detected during admission was recorded, the mean value for which was 1,697 ± 99 cells/μl. The patients were then divided into tertiles based on this value (low: <1,300 cells/μl; medium: 1,300–1,910 cells/μl; and high: >1,910 cells/μl). During the 40-month follow-up period, the total mortality was 9.3% (128 cases), with 3.7% (17 cases) of these in the high tertile, 7% (32 cases) in the medium, and 17.2% (79 cases) in the low lymphocyte tertile (χ^2 $P < 0.001$). Kaplan-Meier survival analysis (Figure 1A) revealed early divergence of the curves, with higher mortality in the low lymphocyte tertile early after discharge and continued divergence throughout the follow-up period ($P < 0.001$). Next, Cox regression analysis was performed with minimum lymphocyte tertile, sex, and age, as well as all baseline variables that significantly differed between minimum lymphocyte tertiles as covariates (Figure 1B and Supplemental Table 1; supplemental material available online with this article; doi:10.1172/JCI80055DS1). This demonstrated that low minimum lymphocyte tertile (low vs. high, hazard ratio [HR] 2.42, 95% CI 1.25–4.71) and increasing age (HR 1.50, 95% CI 1.22–1.84) were both independent predictors of higher mortality in this model, as were higher serum creatinine and a history of angina. The use of a glycoprotein (GP) IIb/IIIa inhibitor during PPCI and higher hemoglobin, on the other hand, were associated with lower mortality. The significant independent predictive effect of lymphopenia was in spite of lower lymphocyte counts in elderly patients (Figure 1C). The difference in the minimum lymphocyte counts recorded between survivors and non-survivors was greatest in patients older than 80 years (Figure 1D), again emphasizing the significance of lymphocyte count independent of age in predicting mortality.

Loss of lymphocytes from circulating blood occurs following reperfusion in STEMI patients. Next, temporal evolution of leukocyte subset counts was studied prospectively following PCI in both STEMI ($n = 59$) and non-ST elevation myocardial infarction (NSTEMI) ($n = 15$) patients (see Table 2 and Figure 2 for details). Characteristic patterns were seen in the STEMI patients, with early depletion of lymphocyte counts compared with the pre-PPCI condition (2,295 ± 129 cells/μl) occurring until 90 minutes (1,317 ± 78 cells/μl), with recovery by 24 hours (2,153 ± 101 cells/μl) (*P* for trend < 0.001, Figure 3A). In contrast, comparable changes were

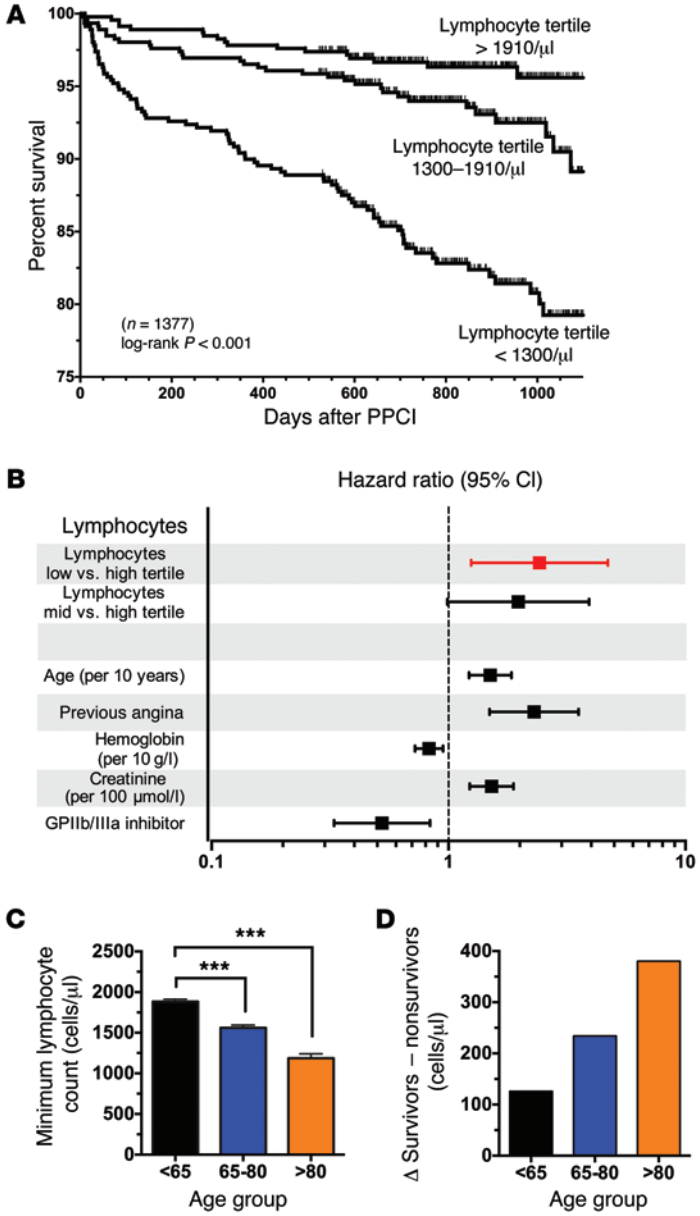

Figure 1. Lymphopenia after PPCI predicts higher mortality after PPCI in STEMI. (**A**) Kaplan-Meier survival curves of 1,377 consecutive patients discharged alive following PPCI (follow up time 1,200 days). Patients were divided into three tertiles according to the minimum peripheral blood lymphocyte counts obtained during their admission. (**B**) Forest plot with outcome of stepwise Cox regression analysis for death over follow-up time, with covariates including age, sex, minimum lymphocyte tertile, previous angina, and serum creatinine (see Supplemental Methods for the full list of covariates) (n = 1,076). (**C**) Minimum lymphocyte count, divided by age group (<65: n = 756, 65–80: n = 472, >80: n = 149) and (**D**) Difference in minimum lymphocyte counts between survivors and non-survivors following PPCI, according to 3 age groups, compared using one-way ANOVA; ***P < 0.001.

not seen in the NSTEMI group (before PCI: 1,899 ± 207 cells/μl, 90 minutes: 1,689 ± 137 cells/μl, P = 0.10). Thus, lymphocyte counts were significantly lower in the STEMI compared with the NSTEMI group at 90 minutes (P = 0.012), although the level was nonsignificantly elevated before PPCI. The temporal evolution of other leukocyte subsets in the STEMI group also showed distinct dynamics. There was a small drop in monocyte counts by 90 minutes (635 ± 36 to 522 ± 28 cells/μl, P = 0.039), followed by a peak at 24 hours (776 ± 36 cells/μl, P = 0.004, Figure 3B). However, no significant differences were observed in monocyte counts between STEMI and NSTEMI patients over the time points studied in both groups. Granulocyte counts, however, were unsurprisingly significantly higher in the STEMI group at each comparable time point (P < 0.001, Figure 3C). They then declined in the STEMI patients between 90 minutes and 24 hours, with a further drop by 3–6 months, at which time this is likely to reflect a steady healthy state (P < 0.001). Within the lymphocyte population, the transient depletion observed after reperfusion in the STEMI group was primarily due to loss of T cells and NK cells. The total T cell count dropped from 1,508 ± 95 cells/μl before reperfusion to 898 ± 58 cells/μl at 90 minutes (P < 0.001, Figure 3D), prior to recovery by 24 hours. In contrast, a significant decline was not seen in the NSTEMI group (1,275 ± 159 cells/μl to 1,234 ± 118 cells/μl, P = 0.11). Similarly, NK cells showed a large drop in the STEMI group, from 501 ± 33 cells/μl to 203 ± 18 cells/μl at 90 minutes (P < 0.001, Figure 3G), although they did not significantly recover by 24 hours. Unlike in T cells, however, the drop in NK cells in the STEMI group was paralleled by a similar, albeit slightly smaller, drop in the NSTEMI group (397 ± 65 to 216 ± 24 cells/μl at 90 minutes, P = 0.004).

Highly differentiated effector T cell subsets show greater decline following reperfusion in STEMI. Having established the transient loss of circulating T cells following reperfusion in STEMI, we focused on the behavior of the subpopulations (Figure 3, E and F, and Figure 4). These were assessed using the percentage change in cell counts, with the total drop best demonstrated by the change occurring between pre-reperfusion and 90 minutes (Figure 4, C and D). While total $CD4^+$ T cell levels dropped by a median of –29% (interquartile range [IQR] –43%, –15%), $CD8^+$ T cells dropped by –55% (IQR –66%, –29%). Comparable drops were not observed in the NSTEMI population (median change of +8% and –3% for $CD4^+$ and $CD8^+$ T cells, respectively; P < 0.001, STEMI vs. NSTEMI for each subset). Furthermore, within these two major T cell subsets, depletion varied between the subpopulations, with a progressively greater drop in the more differentiated cells (Figure 4, C and D). Thus, the effector cells declined by –52% (–67%, –37%) in the case of $CD8^+$ effector memory (T_{EM}) and by –66% (–74%, –44%) in terminally differentiated $CD8^+CD45RA^+$ effector memory (T_{EMRA}) cells, compared with only –26% (–40%, –5%) for $CD8^+$ naive (T_N) cells and –26% (–43%, –6%) for $CD8^+$ central memory (T_{CM}) cells (Figure 4D). A comparable trend was also seen within the equivalent $CD4^+$ T cell subsets (Figure 4C). Moreover, when the effector T cell subsets were further divided by expression of the costimulatory molecule CD27, which is downregulated in highly differentiated T cells, the drop was greater still in cells lacking expression (Supplemental Figure 1). The same pattern in cell level drops was seen in the early post-reperfusion interval between 15 and 30 minutes (Figure 4, A and B). In general, the

Table 2. Baseline data for STEMI and NSTEMI patients included in prospective lymphocyte subpopulation study

	STEMI (*n* = 59)	NSTEMI (*n* = 15)	*P* value
Age	59.3 ± 10.7	61.1 ± 11.8	0.742
Male	44 (74.6)	11 (73.3)	1.000
BMI	26.8 ± 4.6	30.9 ± 6.0	0.006
Diabetes mellitus	6 (10.2)	0 (0)	0.337
Family history of CAD	23 (39.0)	7 (46.7)	0.697
Active smoker	31 (52.5)	4 (26.7)	0.089
Hypertension	19 (32.2)	10 (66.7)	0.020
Anterior MI	28 (47.5)	N/A	N/A
Serum cholesterol (mmol/l)	5.3 ± 1.1	4.3 ± 1.1	0.036
Serum creatinine (μmol/l)	80.2 ± 17.0	84.9 ± 21.4	0.472
Peak troponin T (ng/l)	4899 ± 3385	207 ± 214	<0.001
Procedural characteristics			
Door-to-balloon time (minutes)	26.8 ± 14.3	N/A	N/A
Onset-to-reperfusion time (minutes)	164.6 ± 81.3	N/A	N/A
Onset-to-procedure time (days)	N/A	5.01± 2.78	N/A
Pre PCI flow (TIMI 0/1/2/3)	55/4/0/0	2/1/0/12	<0.001
Post PCI flow (TIMI 0/1/2/3)	0/0/0/59	1/0/0/14	0.203
Vascular access (radial/femoral)	56/3	13/2	0.265
Pre-hospitalization medication			
Statin therapy	10 (16.9)	6 (40.0)	0.077
β-blocker	2 (3.4)	3 (20.0)	0.054
Aspirin	5 (8.5)	2 (13.3)	0.624
ACE inhibitor/ARB	6 (10.2)	7 (46.7)	0.003

Continuous variables expressed as mean ± SD and compared using Mann-Whitney *U* test; categorical variables as *n* (%) and compared using χ^2 or Fisher's exact test as appropriate.

effector T cell subsets (T_{EM} and T_{EMRA}) are known to possess potent effector functions, such as cytokine production, in contrast to the less differentiated T_N and T_{CM} subsets (15).

One potential confounding factor that could have influenced our results was the use of statins before PPCI, given their well-documented antiinflammatory properties (16). Of the 59 patients in the STEMI group, 10 were receiving statins before admission. Interestingly, these patients did have significantly higher lymphocyte and T cell counts at presentation (Supplemental Table 2), although the subsequent percentage changes in leukocyte counts following reperfusion were no different between cases with or without statins (Supplemental Table 3).

Transcoronary gradients suggest loss of T lymphocytes within the myocardial circulation. Given the loss of T lymphocytes from peripheral blood following reperfusion, we investigated whether some of these cells may be sequestered within the reperfused myocardium. In order to assess this, we studied transcoronary gradients, comparing cell counts from blood taken simultaneously from the aorta (proximal to the myocardial vascular tree) and from within the coronary sinus (CS; distal, draining the anterior myocardial bed). There was a significant drop in total T cells (–3.8% ± 0.8%, $P = 0.028$), $CD4^+$ T cells (–3.9% ± 0.8%, $P = 0.028$), and $CD8^+$ T cells (–3.5% ± 1%, $P = 0.027$) across the myocardial circulation in anterior MI when the samples were taken within 45 minutes of reperfusion (Figure 5A). Although these drops in cell counts were small, they were well above the coefficient of variation (CV) of the measurement (1.5%, 1.6%, and 2% for total T cells, $CD4^+$ cells, and $CD8^+$ T cells, respectively; Supplemental Table 4), indicating that they were within the range detectable with this assay. In contrast, in anterior MI cases where the samples were taken later than 45 minutes, and in inferior MI (where the affected myocardium is primarily not drained via the CS), no significant transcoronary gradient was seen (Figure 5B).

Transient depletion of highly differentiated T cell subsets is associated with MVO. Next we investigated whether the changes observed in cell counts were associated with a marker of myocardial I/R injury on cardiac MRI. MVO is known to be one component of I/R injury and can be readily detected on late gadolinium enhancement (LGE) MRI images as an area of hypoenhancement within the infarct core (Figure 6A). To study this phenomenon, we divided STEMI patients into three tertiles based on the presence and extent of MVO (zero, low, and high MVO; see Supplemental Tables 5 and 6 for group characteristics) and compared the dynamic changes in cell counts between each of these tertiles. It was found that the early changes, occurring between 15 and 30 minutes after reperfusion, showed a relationship with the development of MVO (Supplemental Table 7 and Figure 6, C and D). In particular, the early drop in T cell counts demonstrated a very strong association with MVO tertile ($P = 0.003$), with a greater drop in patients with high MVO. In comparison, there was only a weak relationship for monocytes ($P = 0.049$) and none for granulocytes, B cells, or NK cells (Supplemental Table 7). The high-MVO group displayed a significantly greater drop than the zero-MVO group for both $CD4^+$ (–14.3% ± 1.8% vs. –6.0% ± 1.4%, $P = 0.012$) and $CD8^+$ T cells (–27.1% ± 3.6% vs. –13.9% ± 2.5%, $P = 0.020$) (Figure 6, C and D). Furthermore, when the drops in the effector T cell subsets (T_{EM} and T_{EMRA} cells) were analyzed separately, the relationship with MVO was more striking still. In the case of $CD4^+$ T_{EM} cells, the high-MVO group had a mean drop of –21.1% ± 2.3% compared with –8.6% ± 2.1% in the zero-MVO group ($P = 0.005$). The strongest relationship of any cell population, however, was seen in the scarce $CD4^+$ T_{EMRA} cells (high-MVO mean drop: –27.8% ± 3.2% vs. zero-MVO: –7.8 % ± 2.9%, $P < 0.001$). The analysis was also carried out with exclusion of cases with trivial non-physiological (thrombolysis in myocardial infarction [TIMI] grade 1) arterial flow prior to reperfusion in order to assess whether inclusion of these cases affected the results. While significance values were slightly lower due to the smaller case number, the overall findings were unaltered (Supplemental Figure 2). This strong relationship raises the possibility of a mechanistic link between effector T cell depletion following reperfusion and the development of MVO in STEMI. Notably, although the timing of the MRI scans varied between 1 and 8 days after reperfusion, there was no relationship between this timing and the presence of MVO (Supplemental Figure 3), indicating that this was not a source of confounding variation in the MVO data.

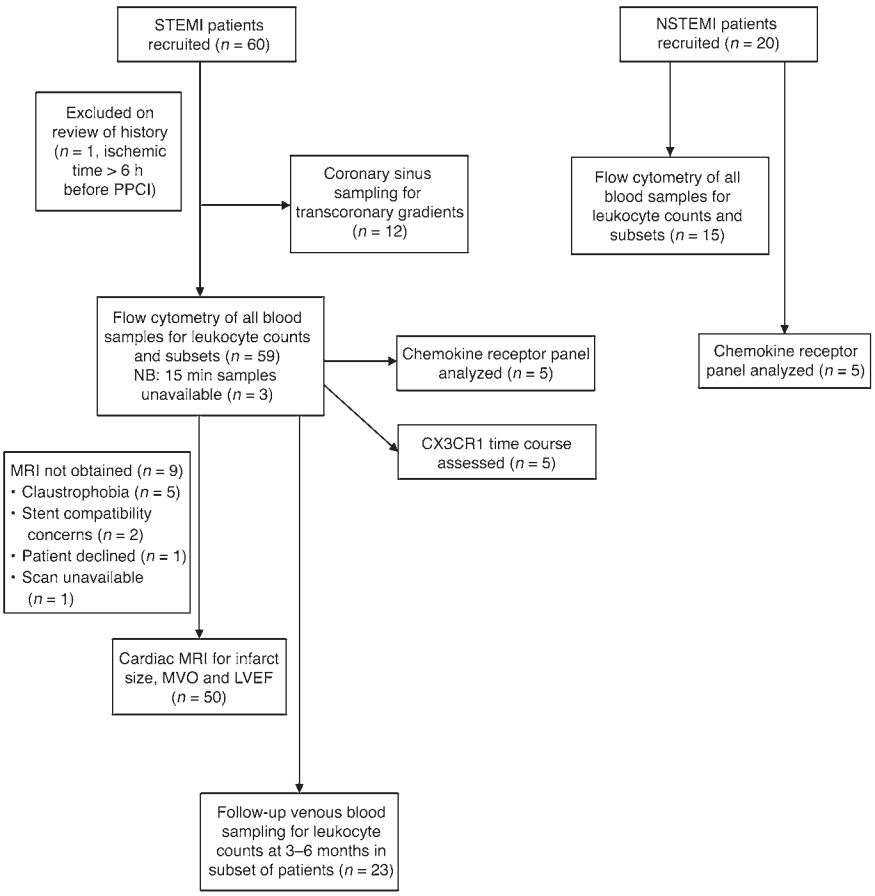

Figure 2. Flow chart for prospective cohort. Study groups recruited and investigations carried out in each.

Moreover, to exclude treatment variation as a potential source of confounding, we confirmed that there was no significant relationship between preadmission statins, antiplatelet agents, or IV antithrombotic treatment during PPCI and any of the MRI parameters recorded, including MVO (Supplemental Table 8).

The chemokine fractalkine and its receptor CX3CR1 follow distinct patterns and are associated with the depletion of lymphocytes following reperfusion in STEMI. Next we wanted to investigate the mechanism behind the observed transient drop in T cell counts. Given that chemokines are critical in leukocyte trafficking in response to ischemia and reperfusion (17), we initially sought to determine the chemokine receptor profile in T cells of patients with coronary heart disease (Figure 7, A and B). First, using flow cytometry we examined the expression of 15 chemokine receptors in patients with NSTEMI undergoing non-emergency PCI (Figure 7A). From this complement we then excluded 5 receptors that appeared unlikely to contribute, given minimal expression in our cells of interest, known alternative unrelated function, and/or lack of published evidence of involvement in myocardial infarction (CCR1, CCR3, CCR6, CCR9, and CXCR5). Expression of the remaining 10 receptors was then assessed acutely in T cell subsets of STEMI patients undergoing PPCI (Figure 7B), and the baseline expression of each receptor was compared with the previously observed transient depletion of these populations following reperfusion (Supplemental Table 9). One receptor, CX3CR1, clearly stood out as showing a strong relationship (r^2 = 0.99, P = 0.006) between expression on T cell subsets and the cellular drop (Supplemental Table 9 and Figure 7C). Moreover, when we analyzed gene transcription for a variety of chemokine and adhesion receptors in peripheral blood mononuclear cells (PBMCs) from STEMI patients undergoing PPCI, the same receptor stood out as showing the most dramatic and consistent change: compared with expression levels 3 months after reperfusion, CX3CR1 was initially downregulated prior to reperfusion, then upregulated 24 hours afterward (Supplemental Table 10). CX3CR1 is the receptor for fractalkine (CX3CL1), a unique chemokine known to play a key role in migration and adhesion of effector T cells and NK cells to vascular endothelium (18, 19). Indeed, expression of CX3CR1 varied significantly between T cell subsets and was higher in $CCR7^-$ effector cells (Figure 7, D and E). Consequently, we then investigated the dynamics of the CX3CR1 ligand soluble fractalkine (sFKN) in the serum of STEMI patients. Despite an initial drop in the first 15 minutes after reperfusion, sFKN reached a peak concentration at 90 minutes, coinciding with the observed nadir in T cell counts (Figure 7F).

Last, we wanted to further assess the interaction between sFKN and CX3CR1 in T cells following reperfusion. We analyzed CX3CR1 expression over time and found a clear initial decrease in CX3CR1 expression in effector $CD4^+$ and $CD8^+$ T cells, prior to partial recovery by 24 hours (Figure 7G). This apparent decrease in CX3CR1 expression could be due to one of three possibilities: cell-by-cell downregulation, selective loss from the bloodstream of CX3CR1-expressing cells, or an interaction with the circulating ligand (sFKN). It was noteworthy that this finding was in contrast to the observed upregulation of CX3CR1 in PBMCs from the gene transcription data (Supplemental Table 10). We speculated that this discrepancy could be related to a ligand-receptor interaction and therefore performed an in vitro competition assay to assess the impact of fractalkine binding on measured CX3CR1 expression. This showed that in CX3CR1-expressing cells, the addition of fractalkine leads to a reduction in CX3CR1 MFI, providing in vitro evidence of ligand-receptor binding and possibly explaining the above discrepancy (Figure 7H).

Discussion

In this study we have shown that lymphopenia during admission is predictive of poor long-term outcome in STEMI treated with PPCI. We have clarified the temporal evolution of lymphocyte dynamics in the blood following reperfusion and shown that lymphopenia in this setting is primarily due to depletion of effector T cell subsets and NK cells. The loss of T cells from the circulation is transient, reaching nadir at 90 minutes, with recovery almost

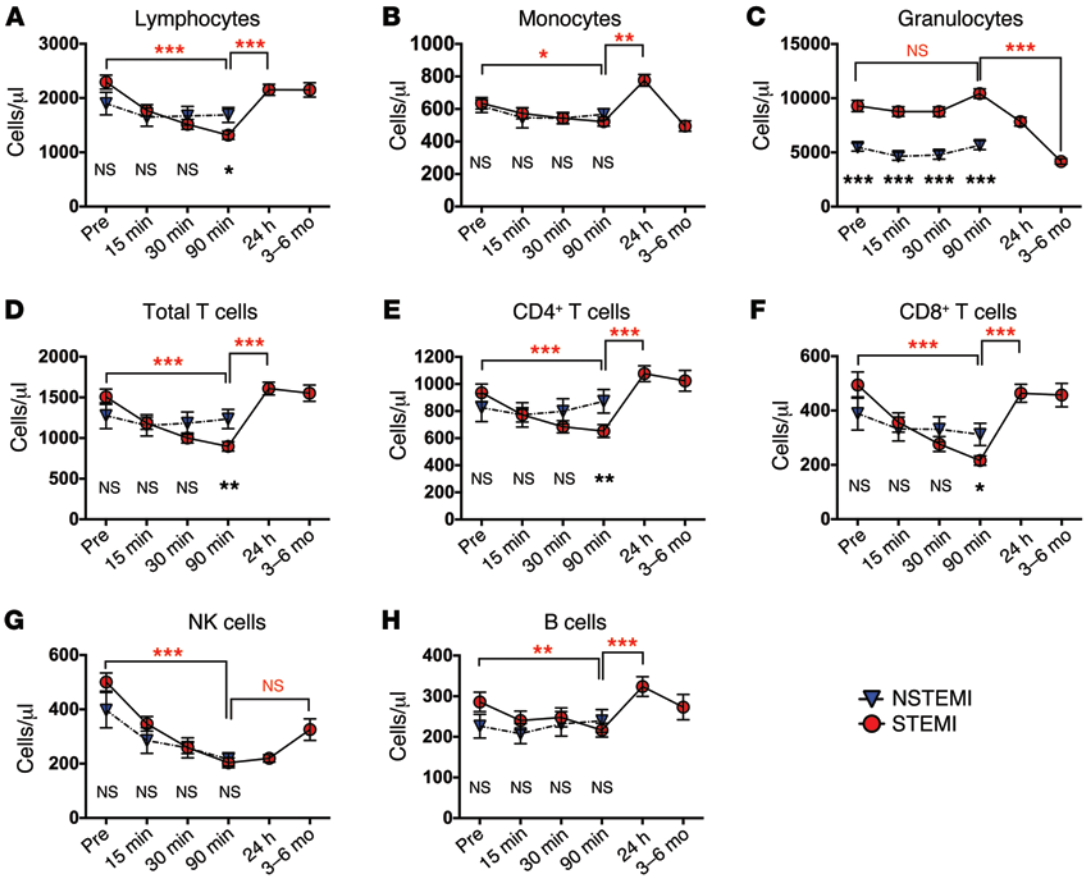

Figure 3. Time courses in circulating leukocyte subset counts. (**A**–**C**) Major leukocyte subsets of (**A**) lymphocytes, (**B**) monocytes, and (**C**) granulocytes, showing change in cell counts over time. Time points were measured from reperfusion in the STEMI group and from first culprit vessel instrumentation (or initial "Pre" blood sampling if no intervention occurred in the NSTEMI group. (**D**–**F**) T lymphocyte cell counts, including (**D**) total T cells, (**E**) $CD4^+$ T cells, and (**F**) $CD8^+$ T cells. (**G** and **H**) $CD3^-$ (non-T) lymphocyte subset counts: (**G**) NK cells and (**H**) B cells. Upper statistics (red) refer to differences in counts between the indicated time points in the STEMI group (Friedman test, with Dunn's multiple-comparisons test); while lower statistics (black) refer to difference between STEMI and NSTEMI at corresponding time points (Mann-Whitney *U* test) (STEMI $n = 59$, NSTEMI $n = 15$). $^*P < 0.05$, $^{**}P < 0.01$, $^{***}P < 0.001$.

complete by 24 hours. Furthermore, we have identified an association between the development of MVO, a component of I/R injury, and the extent of early depletion of effector T cell subsets. This provides what we believe to be the first evidence in humans of a role for these cells in myocardial I/R injury, adding to previously published data from mouse models (6, 7). We have then gone on to elucidate the mechanism of lymphocyte depletion, identifying the chemokine fractalkine as the prime candidate for a central role in this process.

Lymphopenia predicts poor outcome in STEMI treated with PPCI. Until now, the importance of lymphocyte counts in STEMI patients undergoing PPCI has not been fully elucidated. Lymphopenia has previously been shown in a study of 1,037 patients by Dragu et al. to be an independent predictor of long-term mortality in acute myocardial infarction (8). However, this study included both STEMI and NSTEMI patients, managed with a variety of treatment modalities. Furthermore, numerous studies have assessed the predictive value of neutrophil-to-lymphocyte ratio in STEMI treated with PPCI, finding it to be an independent predictor of outcome, in terms of both mortality (13) and major adverse cardiovascular events (10, 12). Our study, however, is the first to our knowledge to directly assess the prognostic significance of lymphocyte counts alone following PPCI for STEMI. We have shown that patients with a lymphocyte count in the lowest tertile have significantly greater mortality over 40 months. Furthermore, while most previous studies have focused on blood tests taken on presentation, we have specifically studied the minimum lymphocyte count observed during the admission. This is of particular relevance, given the significant temporal evolution in lymphocyte counts following reperfusion. Lymphocytes have a critical role in regulating the inflammatory response to tissue damage, through production of both pro- and antiinflammatory cytokines. Thus, it seems likely that the observed association with poor prognosis could be related to their direct involvement in the pathological processes occurring during myocardial infarction and reperfusion.

Transient T cell depletion from the bloodstream is due to selective loss of effector T cells and occurs secondary to I/R. Our data provide clear evidence of lymphocyte depletion from circulating blood following reperfusion, with a detailed analysis of the specific subsets involved. T cell depletion is primarily due to an acute decrease in both $CD4^+$ and $CD8^+$ effector T cells (T_{EM} and T_{EMRA}). In contrast to less differentiated T cell subsets (T_N and T_{CM}), these cells are

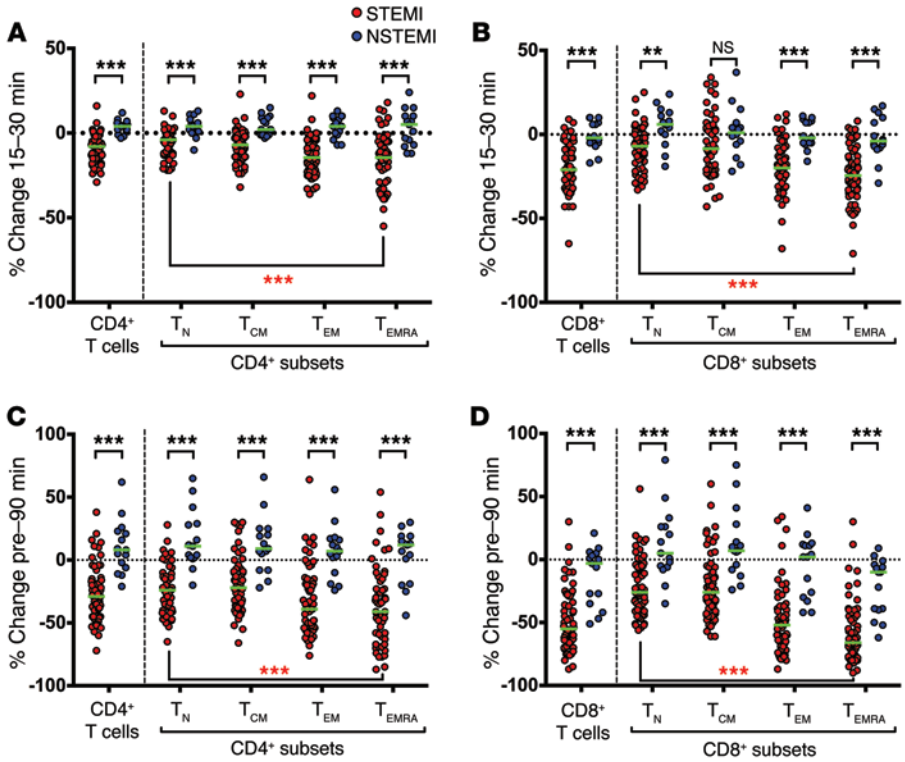

Figure 4. Percentage change in counts of circulating T cell subsets. (**A** and **B**) Changes in T cell subset counts in STEMI (red) and NSTEMI (blue), shown as scatter plots of percentage change between 15 and 30 minutes, in (**A**) $CD4^+$ T cells and subsets and (**B**) $CD8^+$ T cells and subsets. (**C** and **D**) Changes in T cell subset counts between pre-reperfusion and 90 minutes in (**C**) $CD4^+$ T cells and subsets and (**D**) $CD8^+$ T cells and subsets. Median change is indicated by green lines. Upper statistics (black) refer to differences between groups (STEMI and NSTEMI) for each subset (Mann-Whitney *U* test); lower statistics (red) indicate differences between subsets in the STEMI group (Friedman test) (STEMI $n = 59$, NSTEMI $n = 15$). $^{**}P < 0.01$, $^{***}P < 0.001$.

characterized by migration to inflamed tissues and potent effector functions, including production of proinflammatory cytokines such as IFN-γ and TNF-α (15). Importantly, this characteristic loss of effector T cells was seen only in STEMI patients and not in the NSTEMI control group. The NSTEMI and STEMI patients do undoubtedly represent different clinical scenarios, with significantly larger infarcts in the STEMI group and primarily open infarct–related arteries at presentation in the NSTEMI group. Given this latter characteristic, the NSTEMI patients will not have experienced acute I/R. They did, however, undergo the same procedure, and consequently, we believe that this indicates that the characteristic cellular changes seen in the STEMI group were not merely procedurally induced, but were secondary to the I/R process. There are some additional limitations to the use of the NSTEMI group as a control in this setting, most notably the markedly different infarct size, as indicated by the peak troponin T level (Table 2). However, the only potential experiment that could avoid this problem would be to compare STEMI patients undergoing reperfusion with similar cases without reperfusion, which would clearly not be ethically acceptable in a human population.

Our transcoronary gradient data suggest that in STEMI patients following reperfusion, some T cells are lost within the

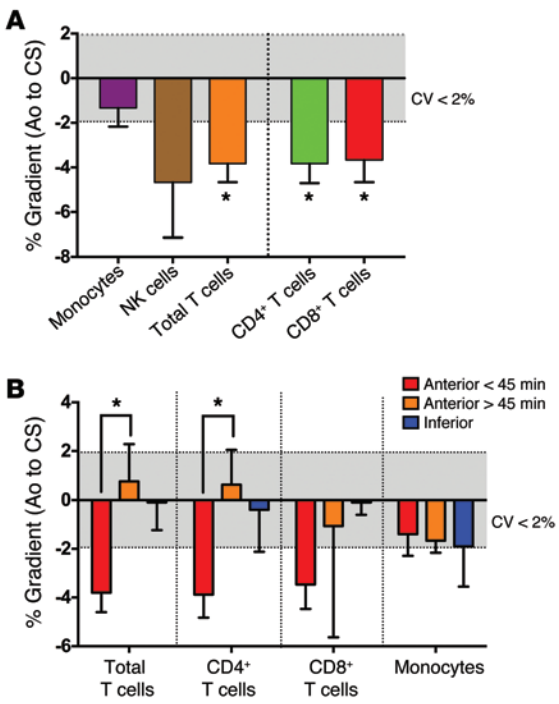

Figure 5. Transcoronary gradients in cell counts, indicating loss of some cells across myocardial circulation. Blood was taken simultaneously from the aortic root and CS at the end of PPCI in a subset of STEMI patients ($n = 12$). Of these, $n = 9$ were anterior STEMI (samples taken at <45 minutes after reperfusion in $n = 6$; >45 minutes after reperfusion in $n = 3$) and $n = 3$ were inferior STEMI (all sampled at <45 minutes). (**A**) Percentage change in cell counts of leukocyte subsets between aorta (Ao) and CS for anterior MI with sampling at <45 minutes ($n = 6$). Negative values indicate a drop across myocardial circulation. Statistics refer to Wilcoxon signed rank test of aorta versus CS counts for the indicated populations. (**B**) Impact of sample timing and infarct location on transcoronary gradients. Statistics refer to difference between anterior infarcts with sampling before ($n = 6$) or after ($n = 3$) 45 minutes (Mann-Whitney *U* test). Note: Mean troponin T for anterior infarcts with sampling <45 minutes: 4,814 ± 1,811 ng/l, anterior infarcts with sampling >45 minutes: 9,705 ± 2,409 ng/l, inferior infarcts: 5,462 ± 2,890 ng/l, excluding larger infarcts in the anterior sampling <45 minutes cases as a possible cause for these findings. $^*P < 0.05$.

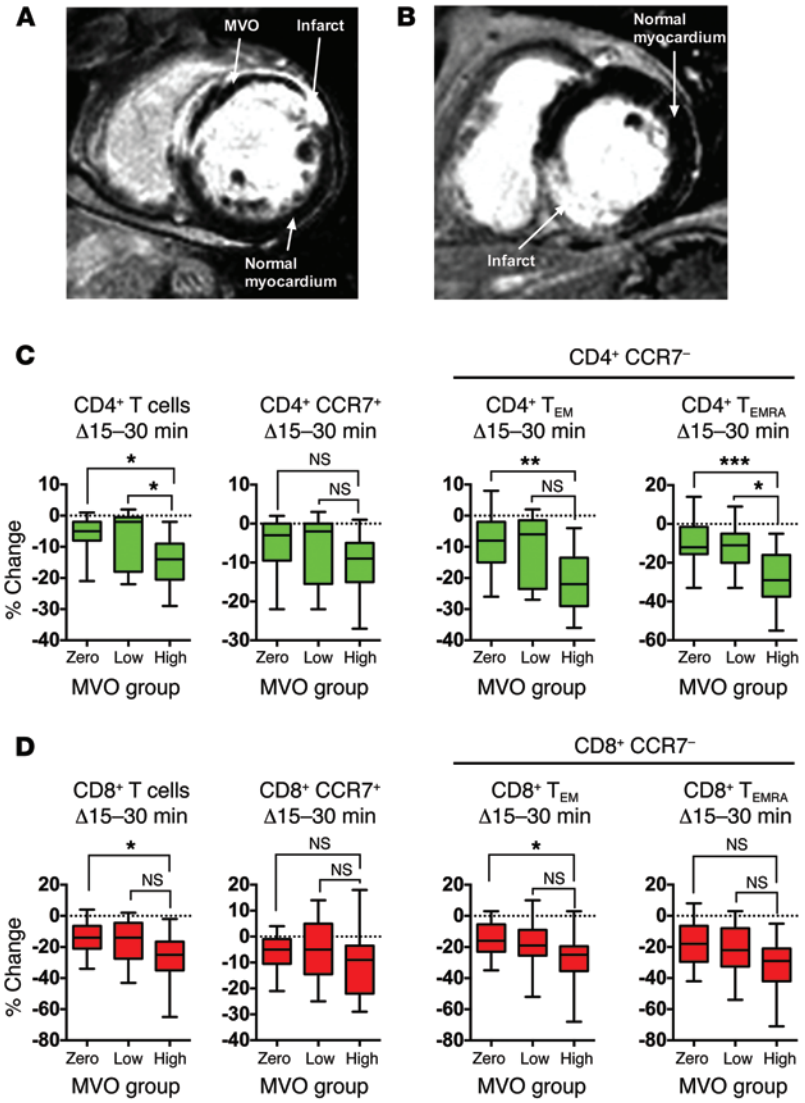

Figure 6. MVO is associated with greater drop in effector T cells. STEMI patients underwent cardiac MRI to detect and quantify MVO. (**A**) Example of anterior MI with MVO. (**B**) Inferior infarct without MVO. STEMI patients were categorized into tertiles based on extent of MVO (zero: $n = 17$, low: $n = 13$, high: $n = 17$). (**C**) Change in cell counts between 15 and 30 minutes after reperfusion for total $CD4^+$ T cells, $CD4^+CCR7^+$ (T_N and T_{CM} combined) cells, and $CD4^+CCR7^-$ effector (T_{EM} and T_{EMRA}) subsets. (**D**) As above for total $CD8^+$ T cells and subsets. Box plots display median (central line), 25th and 75th percentiles (limits of box), and 5th and 95th percentiles (error bars). Statistics refer to differences between MVO groups as indicated (Kruskal-Wallis test with Dunn's multiple-comparisons test) ($n = 47$); $^*P < 0.05$, $^{**}P < 0.01$, $^{***}P < 0.001$.

reperfused myocardial circulation during their depletion from the bloodstream. Consequently, the changes in T cell counts seen exclusively in STEMI patients are likely indicative of recruitment of at least some of these cells into the reperfused myocardium. Moreover, the fact that a significant transcoronary gradient was only seen in anterior STEMI patients when the CS sample was taken within 45 minutes of reperfusion suggests that this sequestration occurs early after reperfusion. Inferior STEMI cases served as a control to demonstrate that transcoronary gradients in T cell counts were only seen when the infarct area vasculature was drained via the CS. However, a limitation of this methodology that must be acknowledged is that while the inferior wall is primarily not drained via the CS, there is considerable anatomical variation. Consequently in certain cases, some of the blood draining from the inferior wall may reach the CS. Nevertheless, no significant T cell transcoronary gradient was seen in the inferior MI cases, despite an infarct size similar to that of anterior cases from whom CS samples were taken early after reperfusion, supporting our conclusions regarding myocardial sequestration of these cells.

Effector T cells are likely to contribute to myocardial I/R injury following PPCI for STEMI. We have shown that greater loss of effector T cells from the circulating blood early after reperfusion is strongly associated with development of MVO, one component of I/R injury, in contrast to primarily negative findings in other leukocyte populations. This further elucidates the work of Bodi et al, who have previously shown an association between lymphopenia after PPCI and MVO (14). The process of MVO is multifactorial, involving direct endothelial damage, leukocyte plugging of the microvasculature, platelet/fibrin embolization, and myocyte swelling (4). Two previous studies have shown an association between neutrophil/lymphocyte ratio (20) and platelet/lymphocyte ratio (21), respectively, and poor myocardial perfusion following PPCI. While our findings demonstrate an association between effector T cell depletion and MVO, they are not conclusive regarding a direct causative relationship. However, taken in the context of previously published research in mice showing a role for IFN-γ–producing $CD4^+$ T cells in myocardial I/R injury (6, 7), we believe this to be the first evidence in humans of such a potential link. We propose that effector T cells may contribute to MVO through direct trapping within the myocardial microvasculature, where they release inflammatory mediators, contributing to further leukocyte infiltration and myocardial damage.

At present, no specific treatment targeting myocardial I/R injury has reached routine clinical use, and most interventions have proved disappointing (22). However, one small proof-of-concept study has shown a potential benefit with administration of cyclosporine immediately prior to PPCI (23). While the rationale for this treatment was prevention of mitochondrial permeability transition pore opening, a key event in I/R injury, it is also noteworthy that it has a profound effect on T cells, limiting their activation through the inhibition of calcineurin (24). It is therefore possible that any beneficial effect in myocardial I/R injury could be mediated at least in part through this mechanism.

Serum fractalkine dynamics and T cell subset CX3CR1 expression suggest a critical role for this chemokine. Fractalkine is a unique chemokine that exists as a membrane-bound adhesion molecule, where it contributes to leukocyte binding and arrest on the vas-

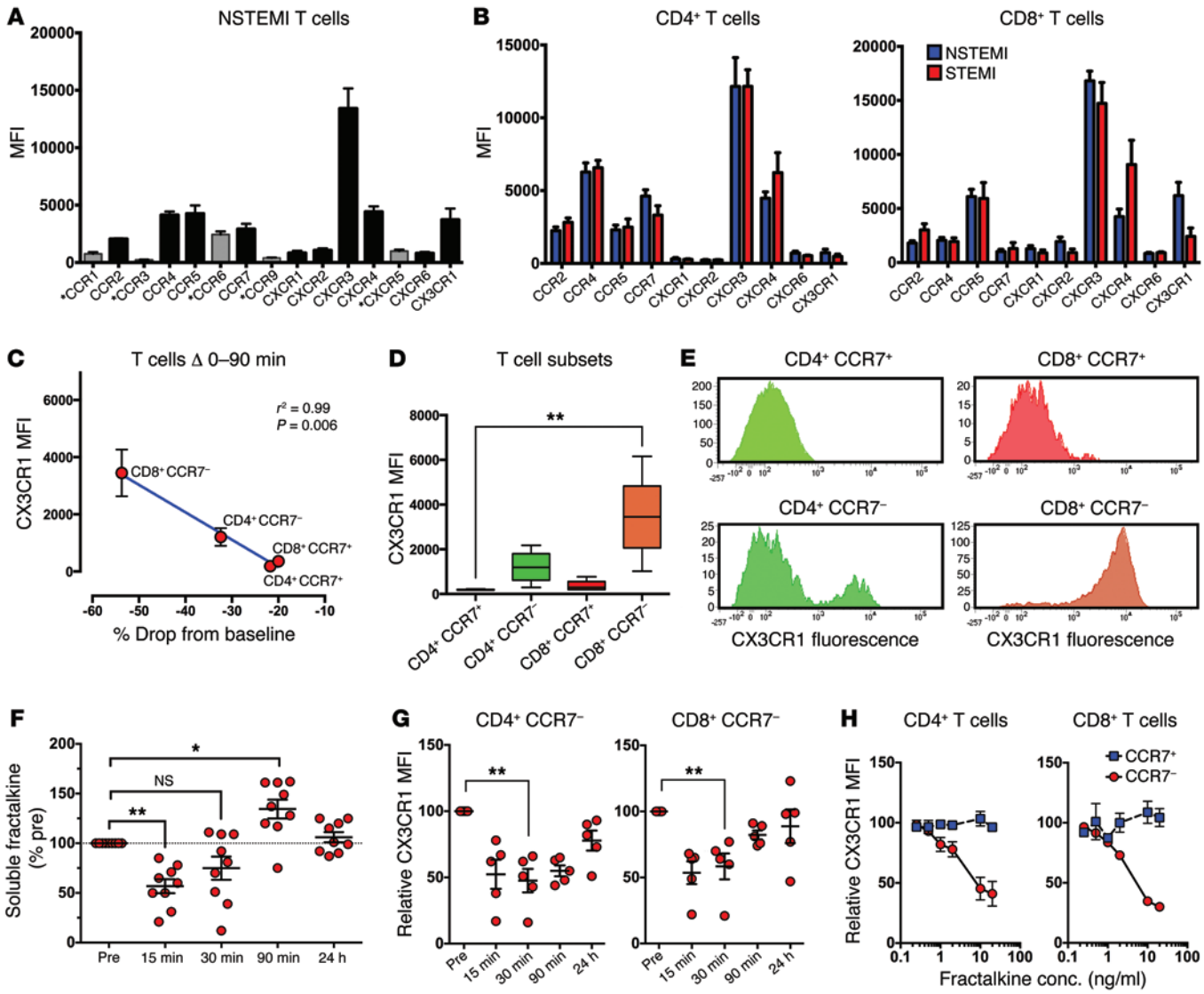

Figure 7. Patterns in expression of the chemokine receptor CX3CR1 and its ligand, fractalkine, suggest a role in T cell dynamics after reperfusion. (**A**) Chemokine receptor expression measured by MFI in T cells in NSTEMI patients (n = 5). Receptors eliminated at this stage indicated by asterisks and gray bars. (**B**) Chemokine receptor expression in CD4$^+$ and CD8$^+$ T cells in NSTEMI (n = 5) and STEMI (n = 5). (**C**) Pre-reperfusion expression of CX3CR1 in T cell subsets (n = 5 subset of STEMI group) correlates strongly with the mean drop in cells in STEMI patients (n = 59), according to linear regression and Pearson correlation coefficient. (**D**) Pre-reperfusion T cell surface expression of CX3CR1 in STEMI patients differs between subsets (Friedman test with Dunn's multiple-comparisons test) (n = 5); box plots show median (central line), 25th and 75th percentiles (box limits), and range (error bars). (**E**) T cell subset CX3CR1 expression histograms (1 representative example of n = 5). (**F**) Serum levels of sFKN in STEMI patients, relative to pre-reperfusion level (one-way ANOVA, with Holm-Šídák multiple comparisons test) (n = 9). (**G**) Surface expression of CX3CR1 in CD4$^+$CCR7$^-$ and CD8$^+$CCR7$^-$ T cells (MFI relative to pre-reperfusion value). The results indicate an apparent drop in expression, which, given the findings in **H**, could also be due to ligand binding (Friedman test with Dunn's multiple-comparisons test) (n = 5). (**H**) Preincubation of blood with recombinant fractalkine prior to CX3CR1 expression analysis indicates competition and reduced fluorescence on CCR7$^-$ (CX3CR1-expressing) T cells (MFI relative to baseline value) (n = 3). *P < 0.05, **P < 0.01. conc., concentration.

cular endothelium, and a soluble secreted form (sFKN) acting as a conventional chemoattractant (19). It is known to contribute to multiple cardiovascular diseases and is thought to have an important role in atherogenesis and plaque destabilization in coronary heart disease (25). Furthermore, it has previously been shown that in the context of chronic cytomegalovirus (CMV) infection, CD4$^+$ T cells are able to induce fractalkine secretion by endothelial cells through production of IFN-γ and TNF-α, inducing further leukocyte recruitment and direct endothelial damage (26, 27). The fractalkine receptor, CX3CR1, stood out among chemokine receptors expressed on lymphocytes as showing a striking correlation between expression in T cell subsets and their depletion from the circulation following reperfusion in STEMI. In keeping with one other study investigating fractalkine levels in this setting (28), we have also shown a peak in sFKN, as well as an increase in gene transcription for CX3CR1, following reperfusion. Prior to this rise in sFKN, however, there was an early drop by 15 minutes after reperfusion. We subsequently demonstrated in vitro evidence of binding between CX3CR1 on the surface of lymphocytes and recombinant soluble fractalkine. We hypothesize

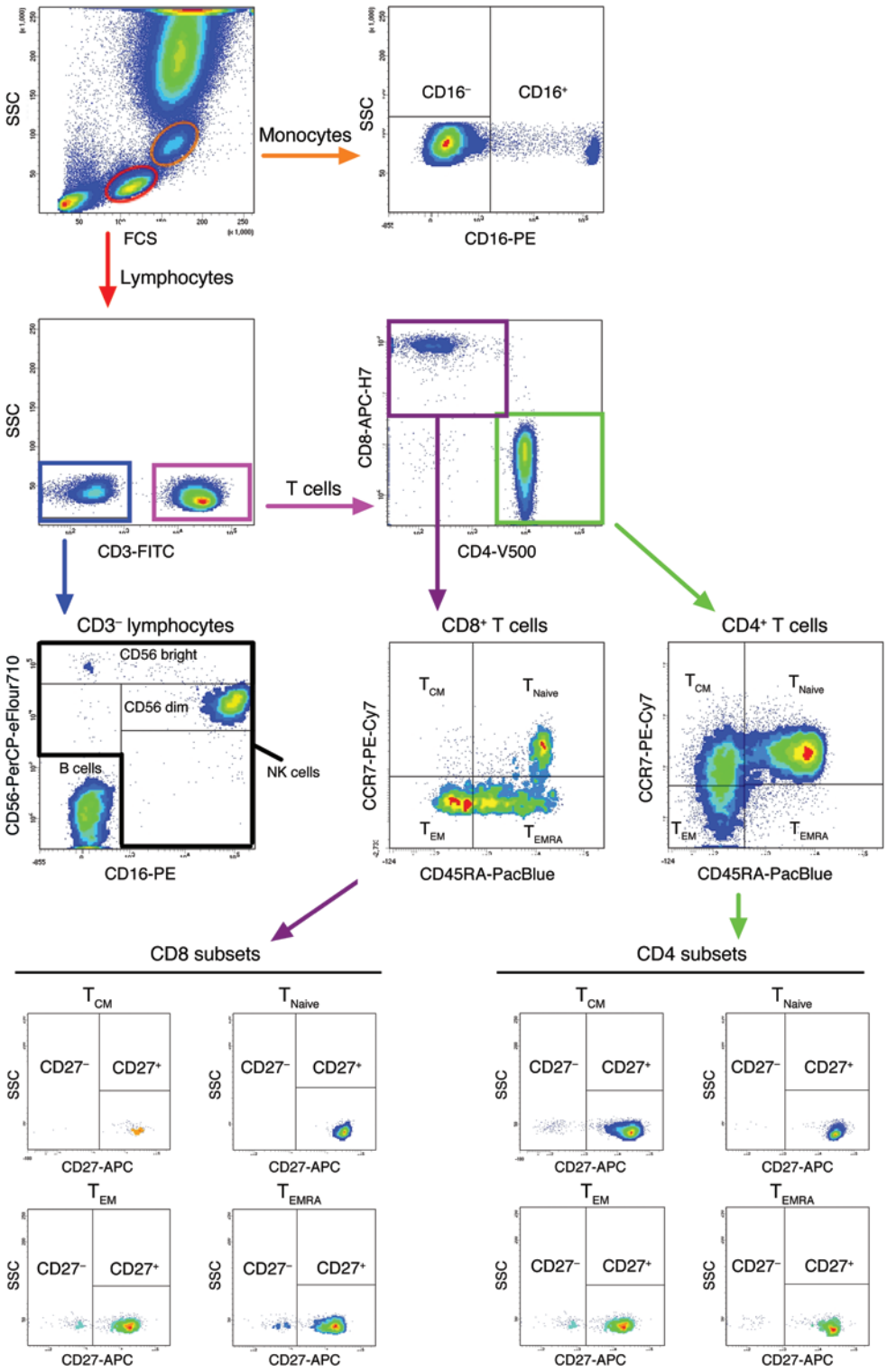

Figure 8. Example of gating strategy for eight-color flow cytometry assay. Lymphocytes and monocytes were gated on their characteristic scatter patterns. Lymphocytes were classified based on CD3 expression to identify T cells, then divided into $CD4^+$ and $CD8^+$ T cells, prior to separation into their four main subsets of naive (T_N), central memory (T_{CM}), effector memory (T_{EM}), and T_{EMRA} cells. Each subset was also analyzed for expression of the differentiation marker CD27. $CD3^-$ lymphocytes were characterized as NK cells or B cells based on expression of CD16 and CD56. Monocytes were subdivided by expression of CD16.

that following reperfusion, any available sFKN is rapidly bound by CX3CR1-expressing leukocytes, many of which also bind membrane-bound fractalkine on inflamed vascular endothelium, resulting in their margination from the circulation. Continued release of sFKN from activated, inflamed endothelium may be augmented secondary to inflammatory cytokine production by effector T cells, leading to the peak seen at 90 minutes, coinciding with the nadir in circulating T cell counts. Furthermore, given the role of fractalkine in leukocyte margination, and the contribution of leukocyte plugging to the development of MVO, it is conceivable that fractalkine-mediated binding of leukocytes to vascular endothelium within the reperfused microcirculation could affect the extent of MVO. This chemokine is known to mediate effector T cell sequestration in a number of other disease processes, including atopic dermatitis (29), rheumatoid arthritis (30), and multiple sclerosis (31), in each of which these cells are

thought to contribute critically to disease mechanisms. Moreover, in an in vitro experimental model using leukocytes from human CMV-positive individuals, stimulated PBMCs have been shown to cause endothelial cell damage in a CX3CR1/fractalkine-dependent manner (27). Leukocyte plugging and endothelial damage are known to be major contributing causes of MVO (4, 32) and represent plausible mechanisms through which T cells could mediate this effect. Release of inflammatory cytokines by effector T cells may also induce further endothelial activation and infiltration of other leukocytes, including neutrophils, compounding the problem. This hypothesis is supported by previously published murine data demonstrating that T cell deficiency in *Rag1*-knockout mice reduces myocardial neutrophil infiltration and protects against I/R injury, while reconstitution with $CD4^+$ T cells able to produce IFN-γ abolishes this protection (7). It is noteworthy, however, that in our study even T cell subsets not expressing CX3CR1 (e.g., $CCR7^+CD4^+$ T cells and B cells) displayed an approximately 20% drop in circulating counts after reperfusion, indicating that signaling through this chemokine receptor is not the sole mechanism behind lymphocyte depletion.

Study limitations. The principal limitations of this study relate to the difficulties in demonstrating causation in disease processes in human subjects. Thus, our findings regarding the relationship between effector T cell dynamics and MVO are correlative in nature. The same limitation affects our findings of a correlation between T cell subset CX3CR1 expression and cellular depletion from the bloodstream following reperfusion. While these studies provide important insights and advance our understanding of the role of T cells in myocardial I/R injury, it must be recognized that we are unable to categorically prove causation through analysis of human patients' samples. To do so would require blockade and reconstitution of an effect in an animal model, for instance through deletion of CX3CR1 or fractalkine in a murine myocardial I/R model. However, such strategies also have substantial disadvantages, most notably the difficulty of achieving a model that suitably replicates the clinical scenario in humans, as well as the significant differences that exist between the human and murine immune systems. Consequently, our study has the advantage of directly investigating the human immune system in the real clinical setting of STEMI treated by PPCI. This allows us to advance our understanding and develop new hypotheses, which can perhaps go on to be tested in animal models. While the involvement of the acquired immune system in myocardial injury and repair is gaining increasing interest (33), it remains significantly underinvestigated, and further studies would be greatly welcomed.

One further possible limitation in our study, however, could be the relatively homogenous total ischemic times of the STEMI population. In order to investigate I/R injury, it was necessary ensure that the total ischemic time was not overly long, with the infarct having already been completed prior to reperfusion. Consequently, the inclusion criteria for our prospective cohort was limited to STEMI patients with total ischemic times of less than 6 hours. Although this was important to ensure an appropriate study sample, it must be borne in mind that in the clinical setting ischemic times are more variable, with patients often presenting later. In such cases it is difficult to be certain whether the findings from our prospective cohort would still apply.

Conclusions. Our results confirm the prognostic significance of lymphopenia following PPCI for STEMI and demonstrate a characteristic pattern of lymphocyte subset depletion following reperfusion. Crucially, our data also suggest a role for effector T cells in the development of MVO and myocardial I/R injury. We have identified the chemokine fractalkine as a prime candidate to have a critical function in this process. The clinical implications of these findings are potentially far reaching. No effective treatment is currently in use to ameliorate I/R injury in patients following PPCI. Our findings identify a potential therapeutic target, opening up a new avenue for further research and future treatment development.

Methods

Supplemental Methods

For further details, see Supplemental Methods.

Retrospective clinical data collection and analysis (cohort 1)

All STEMI patients meeting standard diagnostic criteria and undergoing PPCI (n = 1,531) admitted to a large tertiary center in the United Kingdom between April 2008 and February 2010 were identified retrospectively. Patients with in-hospital mortality were excluded, as were those with acute inflammatory or infectious disease, organ transplantation, or unavailable data, which left a total of 1,377 patients discharged alive and included in the final analysis.

The blood results (complete blood counts) of each patient were identified, and those closest to the time of PPCI and after 24 and 48 hours were recorded, as well as the minimum lymphocyte count during the admission. Mortality data were recorded up to July 2011, giving a follow-up of 40 months (mean 25.2 months).

Survival distributions were estimated using the Kaplan-Meier method and compared using the log-rank test. The effects of known prognostic variables on long-term mortality were examined using Cox proportional hazards regression analysis, using the covariates of sex, age, and minimum lymphocyte tertile, as well as all other baseline variables that differed significantly between groups (for the full list, see Supplemental Methods).

Prospective lymphocyte subset characterization data (cohort 2)

Patient populations and blood sampling. A cohort of 59 STEMI patients were prospectively identified and enrolled in the study at the time of admission. Inclusion criteria were chest pain of onset within 6 hours with new ST segment elevation. Exclusion criteria included cardiogenic shock, previous MI, active infection or malignancy, chronic inflammatory conditions, patent arterial flow in the infarct related artery, and any contraindication to cardiac MRI scanning (for the full list, see Supplemental Methods).

Coronary angiography and PPCI were performed, and arterial blood was acquired at the start of the procedure, then at 15, 30, and 90 minutes following reperfusion. Venous blood was obtained at 24 hours, as well as at 3 to 6 months in a subset of 23 patients.

In a subset of 12 STEMI patients, upon completion of the PPCI procedure and as close to 30 minutes following reperfusion as possible, blood was obtained from the CS via catheterization of the femoral or brachiocephalic vein. Catheter position within the CS was confirmed radiographically by contrast injection. "Simultaneous" aortic blood was obtained via the angioplasty catheter within 30 seconds of CS sampling.

A control group of 15 patients admitted with NSTEMI undergoing non-emergency angiography with or without percutaneous coronary intervention (PCI) were also enrolled. Arterial blood was acquired from these patients at the start of the procedure and at 15, 30, and 90 minutes after culprit vessel instrumentation (or after initial sampling in 4 cases without intervention). A further 5 NSTEMI patients undergoing PCI were subsequently recruited for analysis of lymphocyte chemokine receptor expression.

Enumeration of major leukocyte populations. Blood was obtained as above in 4 ml EDTA tubes (BD Biosciences). Absolute counts of granulocytes, monocytes, total lymphocytes, $CD3^-$ lymphocytes, and T lymphocytes, as well as the major subsets $CD4^+$ and $CD8^+$ T cells, were determined using a four-color BD TruCount flow cytometric assay (BD Biosciences, #342447), as described previously (Supplemental Figure 4, Supplemental Table 4 for CV values for this assay, and ref. 34).

Enumeration of detailed leukocyte subpopulations. Absolute counts of detailed leukocyte subpopulations were determined using an eight-color flow cytometric assay, in conjunction with the major population counts obtained as above. Briefly, 50-μl aliquots of whole blood were stained with a cocktail of the following antibodies: CD3-FITC (clone UCH-T1, #555332), CD4-V500 (clone RPA-T4, #560768), CD8–APC-H7 (clone SK1, #641400), CD16-PE (clone B73.1, #561313), CD27-APC (clone L128, #337169), and CCR7–PE-Cy7 (clone 3D12, #557648) (all BD Biosciences); CD45RA–Pacific Blue (clone MEM-56, #MHCD45RA28, Invitrogen); and CD56–PerCP-eFluor710 (clone CMSSB, #42-0567-42, eBioscience). The samples were then lysed using Pharm Lyse (BD Biosciences) according to the manufacturer's instructions, followed by three wash steps using a BD Lyse Wash Assistant machine (BD Biosciences). Analysis was performed using a BD FACSCanto II machine with FACSDiva software (BD Biosciences). T cell subclassification was carried out based on the established model proposed by Sallusto et al., dividing both $CD4^+$ and $CD8^+$ T cells into naive (T_N), central memory (T_{CM}), effector memory (T_{EM}), and $CD45RA^+$ effector memory (T_{EMRA}) cells (Figure 8 and refs. 15, 35, 36). The cell count for each subset was calculated as the count of the parent population (derived from TruCount assay above) multiplied by the percentage of the parent cells within the subset gate. For CV values for this assay, see Supplemental Table 11.

Serum fractalkine quantification (ELISA). Blood samples were obtained in Vacutainer Serum Tubes (BD Biosciences) and allowed to clot at room temperature. Within 4 hours of collection, serum was separated by centrifugation at 1,000 *g* at room temperature for 10 minutes and stored at –80°C until further analysis. Soluble fractalkine was then measured in serum samples with the ELISA kit (Human CX3CL1/Fractalkine immunoassay, #DCX310, R&D Systems), according to the manufacturer's instructions.

T cell chemokine receptor expression. The surface expression of chemokine receptors in T cells was assessed using a six-color flow cytometric assay. Aliquots of 100 μl whole blood were incubated with a cocktail of the following four antibodies: CD3-PE (clone UCH-T1, #555333), CD4-V400 (clone RPA-T4, #560768), CD8-FITC (clone RPA-T8, #555366) (all BD Biosciences), and CCR7-BV421 (clone G043H7, #353208, BioLegend), as well as an APC-labeled antibody of one of the following specificities: CCR1 (clone 5F10B29, #362908), CCR3 (clone 5E8, #310708), CCR9 (clone L053E8, #358908), CXCR1 (clone 8F1/CXCR1, #320612), CXCR2 (clone 5E8/CXCR2, #320710), CXCR3 (clone G025H7, #353708), or CX3CR1 (clone 2A9-1, #341610) (all BioLegend); and a PE-Cy7–labeled antibody of one of the following specificities: CCR2 (clone K036C2, #357212), CCR4 (clone L291H4, #359420), CCR5 (clone J418F1, #359108), CCR6 (clone G034E3, #353418), CXCR4 (clone 12G5, #306518), CXCR5 (clone J252D4, #356924), or CXCR6 (clone K041E5, #356012) (all BioLegend). Lysis was performed using Pharm Lyse, followed by 3 wash steps as described above). Analysis was then performed on a BD FACSCanto II cytometer, and expression of the each chemokine receptor determined using mean fluorescence intensity (MFI) on the appropriate channel. $CD4^+$ and $CD8^+$ T cells in this assay were further sub-divided into $CCR7^+$ (T_N and T_{CM} combined) and $CCR7^-$ (T_{EM} and T_{EMRA}) cells.

Leukocyte surface CX3CR1 expression in STEMI time-course assay. The time-course of expression of CX3CR1 on leukocyte subsets in STEMI was determined using a six-color flow cytometric assay. Aliquots of 100 μl whole blood were stained with a cocktail of the following antibodies: CD3-FITC (clone UCH-T1, #555332), CD4-V500 (clone RPA-T4, #560768), CD8–APC-H7 (clone SK1, #641400), CD16-PE (clone B73.1, #561313), CD56-PE (clone B159, #555516), CCR7–PE-Cy7 (clone 3D12, #557648) (all BD Biosciences), and CX3CR1-APC (clone 2A9-1, #341610) (BioLegend). Lysis followed by two wash steps was performed as described above. Analysis was performed using a BD FACSCanto II machine, with expression of CX3CR1 for each population determined using MFI on the APC channel.

When this assay was performed with fractalkine preincubation to assess CX3CR1 binding, 100 μl donor blood was incubated for 1 hour at room temperature with the indicated concentration of the recombinant fractalkine standard included with the above ELISA kit (#DCX310, R&D Systems), prior to surface antibody staining as above.

PBMC isolation. PBMCs were isolated by density gradient centrifugation, cryopreserved, and stored at –80°C as previously described (34).

Real-time RT-PCR. Total RNA was extracted from cryopreserved PBMCs of STEMI patients with TRIzol solution (Life Technologies). Total RNA (up to 1 μg) was reverse transcribed using the High Capacity cDNA Reverse Transcription Kit (Life Technologies) according to the manufacturer's instructions. The resulting cDNA samples were stored at –80°C. For TaqMan real-time RT-PCR of *CX3CR1*, *CXCR4*, and *18S* RNA, up to 400 ng of cDNA was used for each reaction. The following TaqMan Gene Expression Assays (Life Technologies) were mixed with patients' cDNA: 18s (Hs03003631_g1), CX3CR1 (Hs01922583_s1), and CXCR4 (Hs00607978_s1). Real-time RT-PCR reactions were carried out in 96-well reaction plates in a volume of 20 μl using TaqMan Universal Master Mix (Life Technologies). Reaction plates were run on the Applied Biosystems 7500HT Fast Real-Time PCR System with the following profile: 95°C for 20 seconds, followed by 40 cycles of 95°C for 3 seconds and 60°C for 30 seconds. The relative expression of each gene in the different tissues was calculated by the ΔΔCT comparative expression method, and the ΔCT values for all the genes in each sample were calculated by subtracting the mean CT values for the housekeeping gene (*18S*) from the CT value for each target gene.

Cardiac MRI. MRI scans were obtained at 1–8 days after infarction with a Siemens Avanto 1.5 Tesla MRI scanner, using a phased array body coil. All images were obtained during breath-holding. Cine images were obtained in parallel short axis slices covering the full extent of the left ventricle, as well as vertical and horizontal long axis, and three chamber views, using a steady-state free precession pulse (SSFP) sequence (repetition time [TR]: set according to heart rate, echo time [TE]: 1.19 ms, flip angle: 80°, field of view [FOV]: 255 ×

340 mm, image matrix: 144 × 192). Corresponding end-diastolic short axis LGE images were obtained using an inversion recovery (IR) segmented gradient echo sequence (TR: according to heart rate, TE: 3.41 ms, flip angle: 25°, FOV: 255 × 340 mm, matrix: 192 × 256) 10 minutes after administration of gadobutrol contrast (Gadovist, Bayer Schering Pharma) at a dose of 0.1 mmol/kg. The inversion time (TI) was selected and adjusted throughout to null normal myocardium.

Image analysis was performed using validated cardiac MRI analysis software (cvi[42], Circle Cardiovascular Imaging Inc.) by an individual blinded to cellular data. Following visual identification of the limits of the left ventricular (LV) cavity, epicardial and endocardial borders were traced automatically on each end-systolic and end-diastolic short axis cine frame, with manual correction where necessary, allowing calculation of LV mass, dimensions, and ejection fraction (LVEF). Epicardial and endocardial borders were then traced on each LGE slice, and areas of enhancement (infarction) identified and quantified automatically using a signal intensity threshold of 5 SDs above normal remote myocardium, as previously described and validated (37). Regions of hypoenhancement within the enhanced zone (MVO) were identified and quantified using semiautomatic thresholding following manual border delineation of areas of interest, and included in the calculated infarct mass.

Statistics

All statistical analysis was performed using SPSS (version 21; IBM), and graphs were produced in GraphPad Prism (version 6). Where data did not pass normality testing by Shapiro-Wilk test, nonparametric tests were used. Nonparametric correlations between parameters were assessed using Spearman correlation coefficient. Unmatched groups were compared using Mann-Whitney *U* test (two groups) or Kruskal-Wallis test with Dunn's multiple-comparisons test (three or more groups). Matched groups (three or more) were compared using Friedman's test with Dunn's multiple-comparisons test. Where normality testing criteria were met, three or more groups were compared using one-way ANOVA with Holm-Šídák multiple-comparisons test. Data are expressed as mean ± SEM unless otherwise stated. Where multiple comparison tests were used, reported *P* values are those corrected for multiple tests. A *P* value of less than 0.05 was considered significant.

Study approval

For the prospective component, ethical approval was obtained from the National Research Ethics Service Committee North East (REC ref. 12/NE/0322). The study was conducted according to the principles set out in the Declaration of Helsinki. Written informed consent was obtained from all prospective patients.

Acknowledgments

B. Keavney is supported by a British Heart Foundation Personal Chair.

Address correspondence to: Ioakim Spyridopoulos, Professor of Cardiology, Chair of Cardiovascular Gerontology, Institute of Genetic Medicine, Newcastle University, Central Parkway, Newcastle upon Tyne, NE1 3BZ, United Kingdom. Phone: 44.191.2418675; E-mail: ioakim.spyridopoulos@newcastle.ac.uk.

1. Yellon DM, Hausenloy DJ. Myocardial reperfusion injury. *N Engl J Med*. 2007;357(11):1121–1135.
2. Hausenloy DJ, Ong SB, Yellon DM. The mitochondrial permeability transition pore as a target for preconditioning and postconditioning. *Basic Res Cardiol*. 2009;104(2):189–202.
3. Vinten-Johansen J. Involvement of neutrophils in the pathogenesis of lethal myocardial reperfusion injury. *Cardiovasc Res*. 2004;61(3):481–497.
4. Ito H. No-reflow phenomenon in patients with acute myocardial infarction: its pathophysiology and clinical implications. *Acta Med Okayama*. 2009;63(4):161–168.
5. Huang Y, Rabb H, Womer KL. Ischemia-reperfusion and immediate T cell responses. *Cell Immunol*. 2007;248(1):4–11.
6. Yang Z, et al. Infarct-sparing effect of A2A-adenosine receptor activation is due primarily to its action on lymphocytes. *Circulation*. 2005;111(17):2190–2197.
7. Yang Z, et al. Myocardial infarct-sparing effect of adenosine A2A receptor activation is due to its action on $CD4^+$ T lymphocytes. *Circulation*. 2006;114(19):2056–2064.
8. Dragu R, et al. Predictive value of white blood cell subtypes for long-term outcome following myocardial infarction. *Atherosclerosis*. 2008;196(1):405–412.
9. Cho KH, et al. Value of early risk stratification using hemoglobin level and neutrophil-to-lymphocyte ratio in patients with ST-elevation myocardial infarction undergoing primary percutaneous coronary intervention. *Am J Cardiol*. 2011;107(6):849–856.
10. Han YC, et al. Neutrophil to lymphocyte ratio predicts long-term clinical outcomes in patients with ST-segment elevation myocardial infarction undergoing primary percutaneous coronary intervention. *Korean Circ J*. 2013;43(2):93–99.
11. Horne BD, et al. Which white blood cell subtypes predict increased cardiovascular risk? *J Am Coll Cardiol*. 2005;45(10):1638–1643.
12. Kaya MG, et al. Prognostic value of neutrophil/lymphocyte ratio in patients with ST-elevated myocardial infarction undergoing primary coronary intervention: a prospective, multicenter study. *Int J Cardiol*. 2013;168(2):1154–1159.
13. Shen XH, Chen Q, Shi Y, Li HW. Association of neutrophil/lymphocyte ratio with long-term mortality after ST elevation myocardial infarction treated with primary percutaneous coronary intervention. *Chin Med J (Engl)*. 2010;123(23):3438–3443.
14. Bodí V, et al. Post-reperfusion lymphopenia and microvascular obstruction in ST-segment elevation acute myocardial infarction. *Rev Esp Cardiol*. 2009;62(10):1109–1117.
15. Sallusto F, Geginat J, Lanzavecchia A. Central memory and effector memory T cell subsets: function, generation, and maintenance. *Annu Rev Immunol*. 2004;22:745–763.
16. Antonopoulos AS, Margaritis M, Lee R, Channon K, Antoniades C. Statins as anti-inflammatory agents in atherogenesis: molecular mechanisms and lessons from the recent clinical trials. *Curr Pharm Des*. 2012;18(11):1519–1530.
17. Frangogiannis NG. Chemokines in ischemia and reperfusion. *Thromb Haemost*. 2007;97(5):738–747.
18. Dimitrov S, Benedict C, Heutling D, Westermann J, Born J, Lange T. Cortisol and epinephrine control opposing circadian rhythms in T cell subsets. *Blood*. 2009;113(21):5134–5143.
19. Umehara H, Bloom ET, Okazaki T, Nagano Y, Yoshie O, Imai T. Fractalkine in vascular biology: from basic research to clinical disease. *Arterioscler Thromb Vasc Biol*. 2004;24(1):34–40.
20. Akpek M, et al. Relation of neutrophil/lymphocyte ratio to coronary flow to in-hospital major adverse cardiac events in patients with ST-elevated myocardial infarction undergoing primary coronary intervention. *Am J Cardiol*. 2012;110(5):621–627.
21. Kurtul A, et al. Usefulness of the platelet-to-lymphocyte ratio in predicting angiographic reflow after primary percutaneous coronary intervention in patients with acute ST-segment elevation myocardial infarction. *Am J Cardiol*. 2014;114(3):342–347.
22. Hausenloy DJ, Yellon DM. Myocardial ischemia-reperfusion injury: a neglected therapeutic target. *J Clin Invest*. 2013;123(1):92–100.
23. Piot C, et al. Effect of cyclosporine on reperfusion injury in acute myocardial infarction. *N Engl J Med*. 2008;359(5):473–481.
24. Azzi JR, Sayegh MH, Mallat SG. Calcineurin inhibitors: 40 years later, can't live without.

J Immunol. 2013;191(12):5785–5791.
25. Damås JK, et al. Expression of fractalkine (CX3CL1) and its receptor, CX3CR1, is elevated in coronary artery disease and is reduced during statin therapy. *Arterioscler Thromb Vasc Biol*. 2005;25(12):2567–2572.
26. Bolovan-Fritts CA, Trout RN, Spector SA. Human cytomegalovirus-specific $CD4^+$-T-cell cytokine response induces fractalkine in endothelial cells. *J Virol*. 2004;78(23):13173–13181.
27. Bolovan-Fritts CA, Spector SA. Endothelial damage from cytomegalovirus-specific host immune response can be prevented by targeted disruption of fractalkine-CX3CR1 interaction. *Blood*. 2008;111(1):175–182.
28. Njerve IU, Solheim S, Lunde K, Hoffmann P, Arnesen H, Seljeflot I. Fractalkine levels are elevated early after PCI-treated ST-elevation myocardial infarction; no influence of autologous bone marrow derived stem cell injection. *Cytokine*. 2014;69(1):131–135.
29. Staumont-Sallé D, et al. CX_3CL1 (fractalkine) and its receptor CX_3CR1 regulate atopic dermatitis by controlling effector T cell retention in inflamed skin. *J Exp Med*. 2014;211(6):1185–1196.
30. Nanki T, et al. Migration of CX3CR1-positive T cells producing type 1 cytokines and cytotoxic molecules into the synovium of patients with rheumatoid arthritis. *Arthritis Rheum*. 2002;46(11):2878–2883.
31. Broux B, et al. CX(3)CR1 drives cytotoxic CD4(+) CD28(–) T cells into the brain of multiple sclerosis patients. *J Autoimmun*. 2012;38(1):10–19.
32. Schwartz BG, Kloner RA. Coronary no reflow. *J Mol Cell Cardiol*. 2012;52(4):873–882.
33. Hofmann U, Frantz S. Role of lymphocytes in myocardial injury, healing, and remodeling after myocardial infarction. *Circ Res*. 2015;116(2):354–367.
34. Hoffmann J, et al. High-throughput 13-parameter immunophenotyping identifies shifts in the circulating T-cell compartment following reperfusion in patients with acute myocardial infarction. *PLoS One*. 2012;7(10):e47155.
35. Koch S, Larbi A, Derhovanessian E, Ozcelik D, Naumova E, Pawelec G. Multiparameter flow cytometric analysis of CD4 and CD8 T cell subsets in young and old people. *Immun Ageing*. 2008;5:6.
36. Sallusto F, Lenig D, Förster R, Lipp M, Lanzavecchia A. Two subsets of memory T lymphocytes with distinct homing potentials and effector functions. *Nature*. 1999;401(6754):708–712.
37. Vermes E, Childs H, Carbone I, Barckow P, Friedrich MG. Auto-threshold quantification of late gadolinium enhancement in patients with acute heart disease. *J Magn Reson Imaging*. 2013;37(2):382–390.